Electronic Supplementary Material (ESI) for Physical Chemistry Chemical Physics.

Supporting Information

Insights into the baicalein-induced destabilization of LS-shaped $A\beta_{42}$ protofibril using computer simulations

Gagandeep Kaur,[a]§ Opinder Kaur Mankoo,[a]§ Anupamjeet Kaur,[a]# Deepti Goyal*[b] and Bhupesh Goyal*[c]

[a] Department of Chemistry, Faculty of Basic and Applied Sciences, Sri Guru Granth Sahib World University, Fatehgarh Sahib-140406, Punjab, India

[b] Department of Chemistry, DAV College, Sector 10, Chandigarh-160011, India

[c] Department of Chemistry & Biochemistry, Thapar Institute of Engineering & Technology, Patiala-147004, Punjab, India

*Corresponding author

Email address: deeptig@iitbombay.org; bhupesh@iitbombay.org

§Both authors contributed equally in this manuscript.

#Present address

National Institute of Immunology, Aruna Asaf Ali Marg, New Delhi–110067, India

List of contents

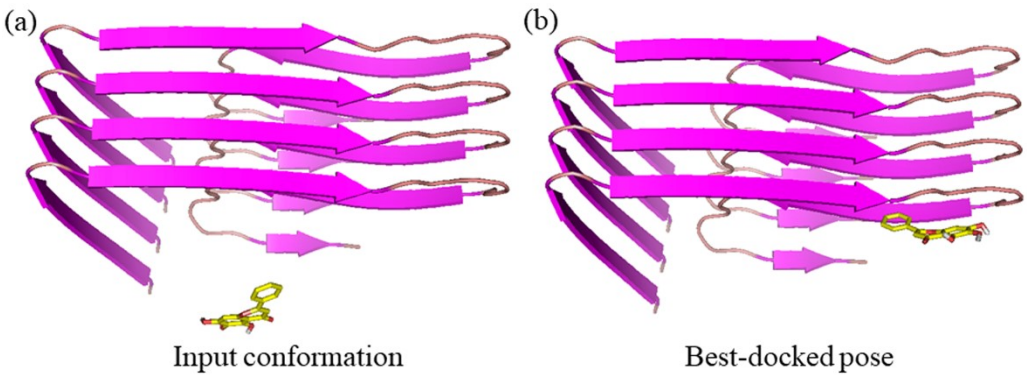

Figure S1: Input conformation of $A\beta_{42}$ protofibril and baicalein for the molecular docking (panel a). The best-docked pose of baicalein with $A\beta_{42}$ protofibril (panel b). The $A\beta_{42}$ protofibril is shown in the cartoon and baicalein is displayed in the stick representation.

Docked pose	Binding energy (kcal/mol)	Docked conformation	Docked pose	Binding energy (kcal/mol)	Docked conformation
1	–6.9	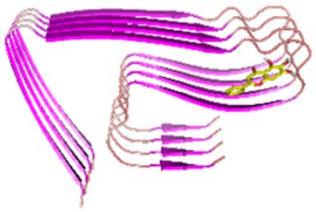	6	–5.8	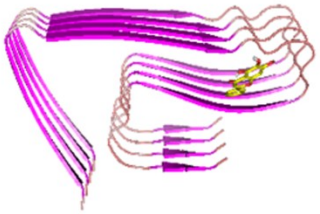
2	–6.2	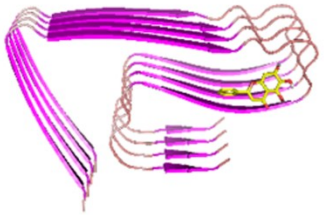	7	–5.6	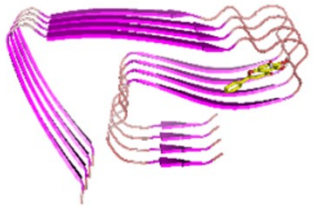
3	–6.0	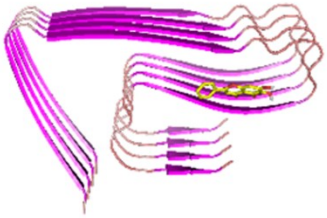	8	–5.5	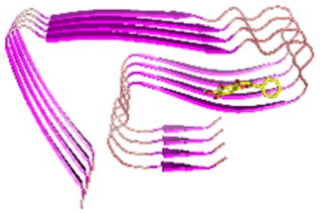
4	–5.9	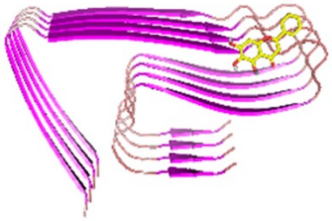	9	–5.4	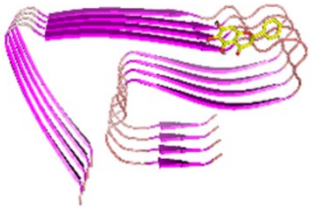
5	–5.8	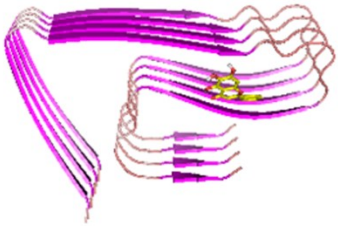			

Figure S2: Top nine docked conformations of baicalein with $A\beta_{42}$ protofibril.

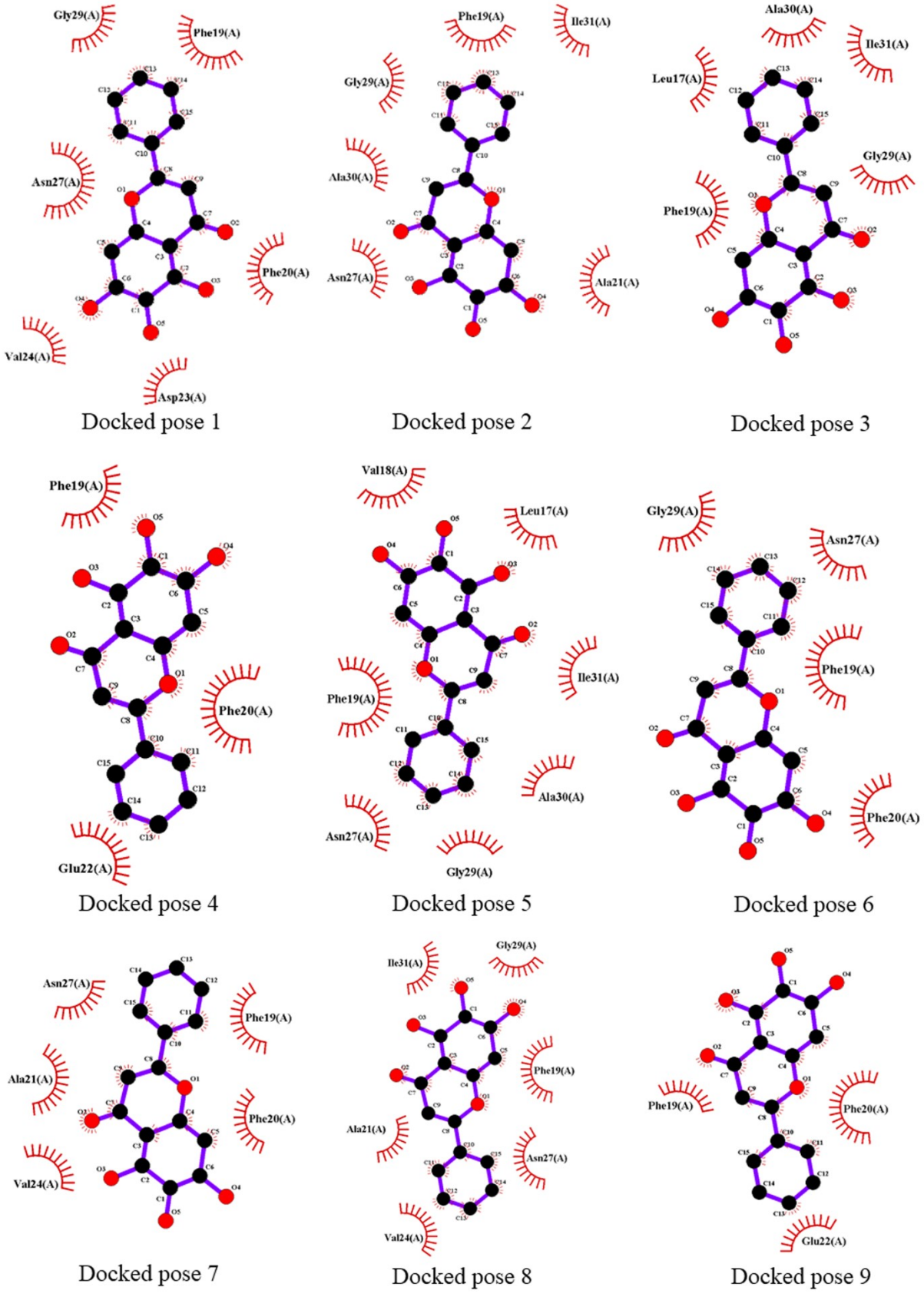

Figure S3: 2D interaction maps displaying hydrophobic contacts of baicalein with $A\beta_{42}$ protofibril in the top nine docked conformations.

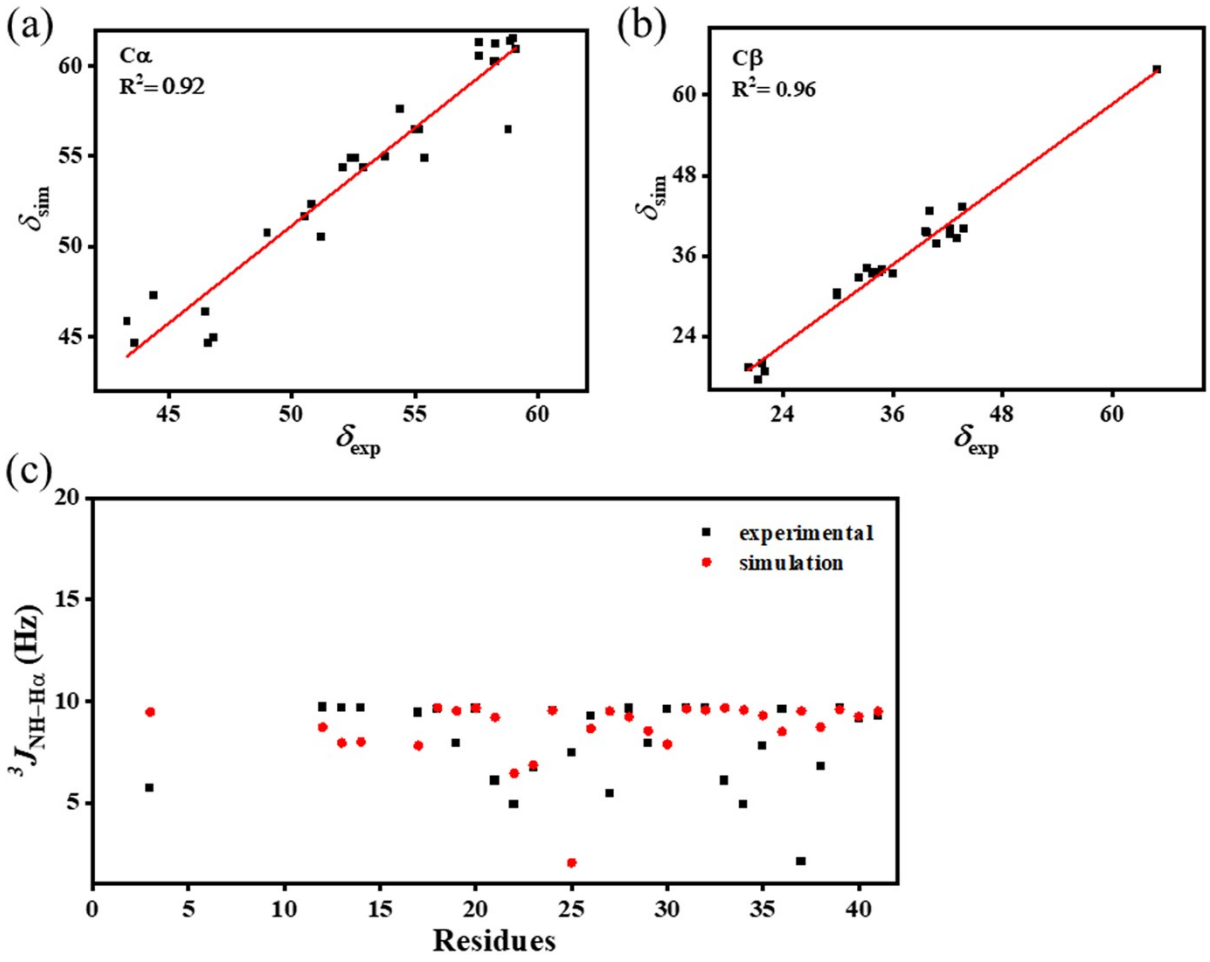

Figure S4: Comparison of NMR chemical shifts of Cα (panel a) and Cβ (panel b) atoms, $^{3}J_{NH-H\alpha}$ coupling constants (panel c) of $A\beta_{42}$ protofibril residues with the simulation data.

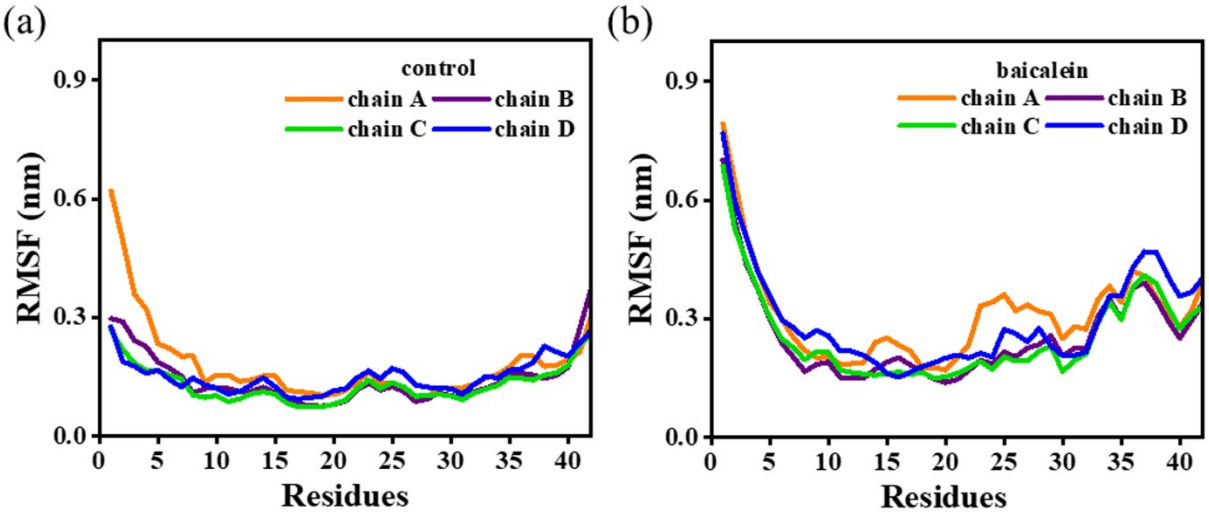

Figure S5: Chain-wise RMSF of $A\beta_{42}$ protofibril residues in the control and baicalein system are shown in panels a, and b, respectively.

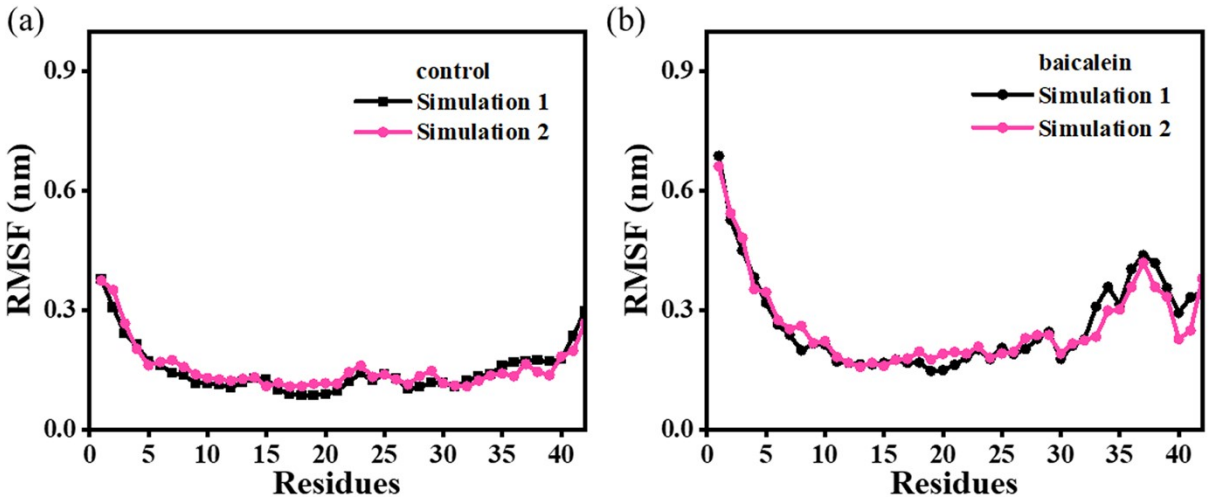

Figure S6: Variations in the RMSF with simulation time for the repeat simulations with varying initial velocities in the control and baicalein systems is shown in panel a, and b, respectively.

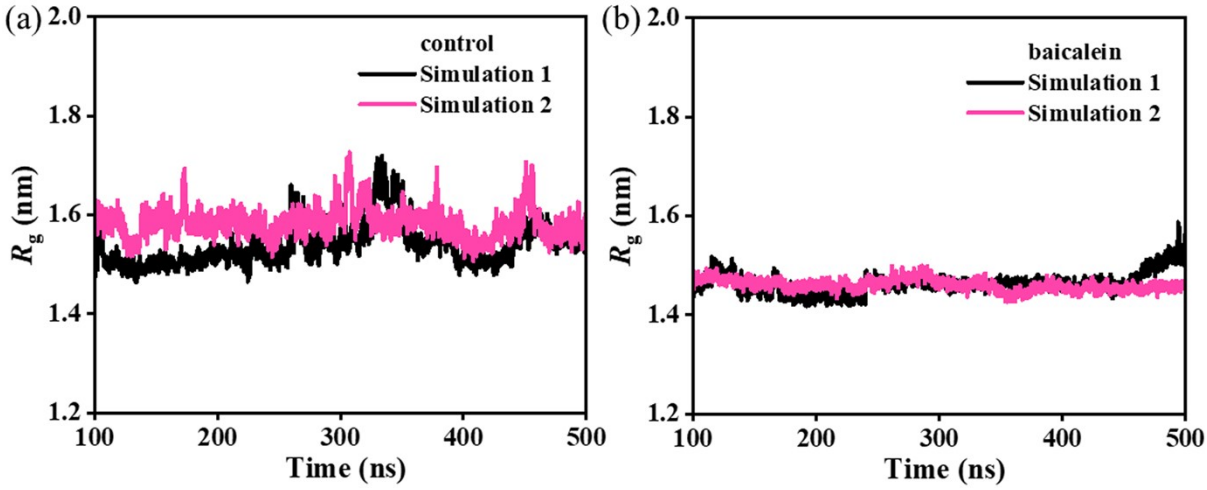

Figure S7: Variations in the R_g with simulation time for the repeat simulations with varying initial velocities in the control and baicalein systems is shown in panel a, and b, respectively.

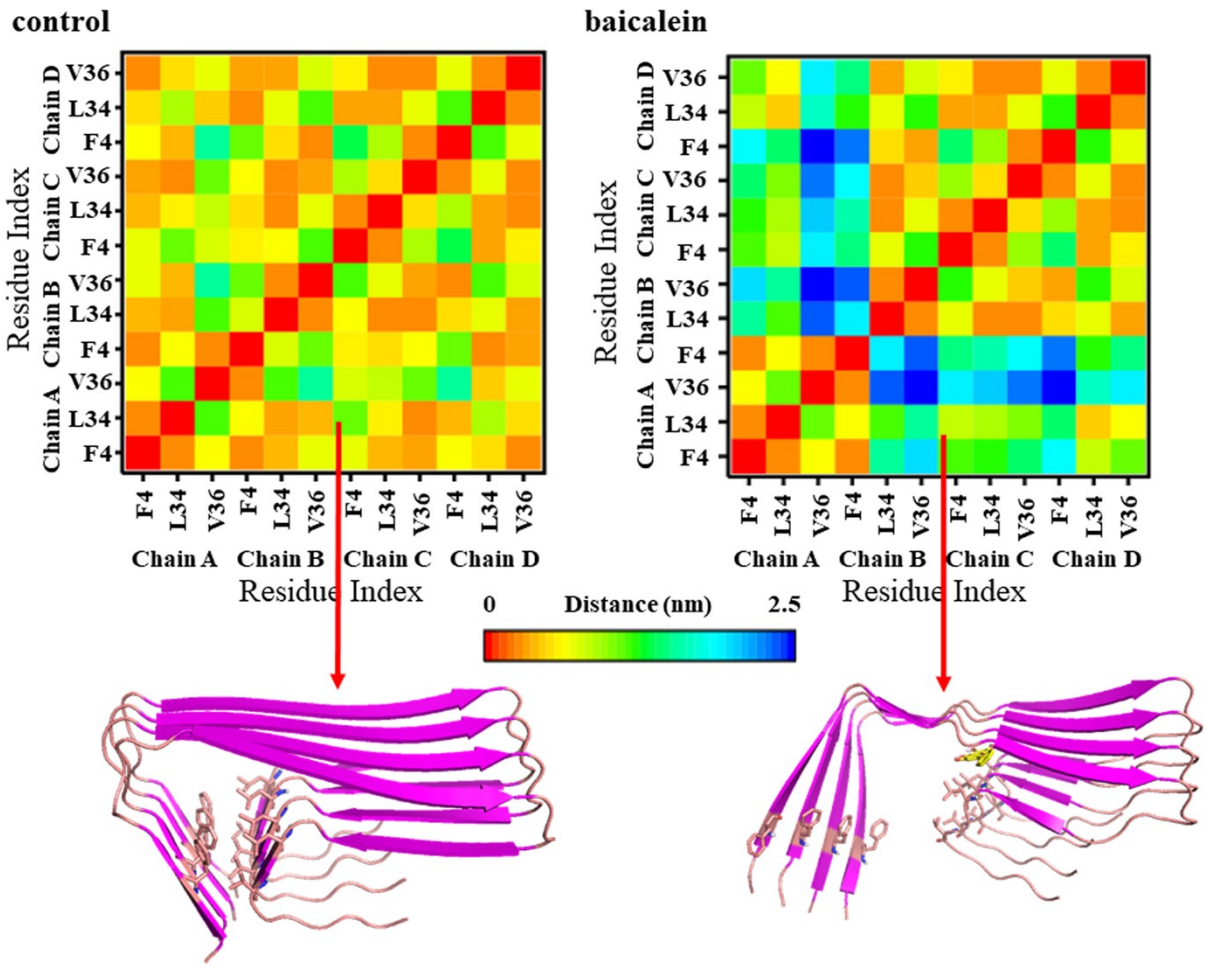

Figure S8: Contact maps displaying the disruption of side-chain contacts within the hydrophobic core (F4, L34 and V36) of 5OQV structure on the inclusion of baicalein. The conformational snapshots shown underneath contact maps depicts the structural deformation in 5OQV structure due to the disruption of hydrophobic contacts between F4, L34 and V36 residues.

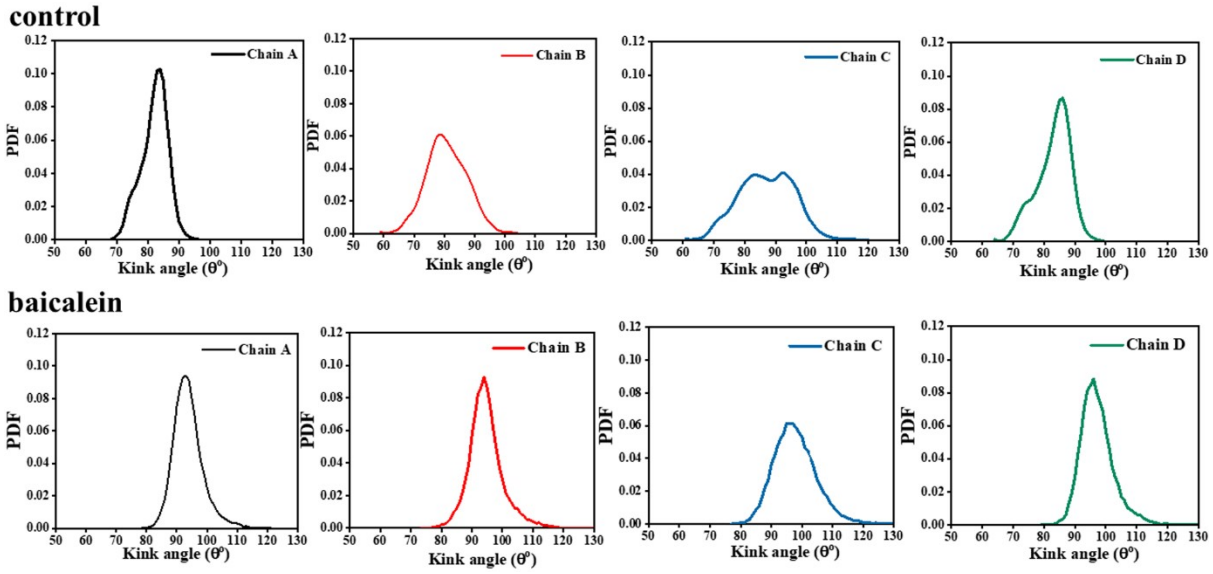

Figure S9: Distribution of kink angle for each chain of the protofibril in control (upper panel) and baicalein (lower panel) systems.

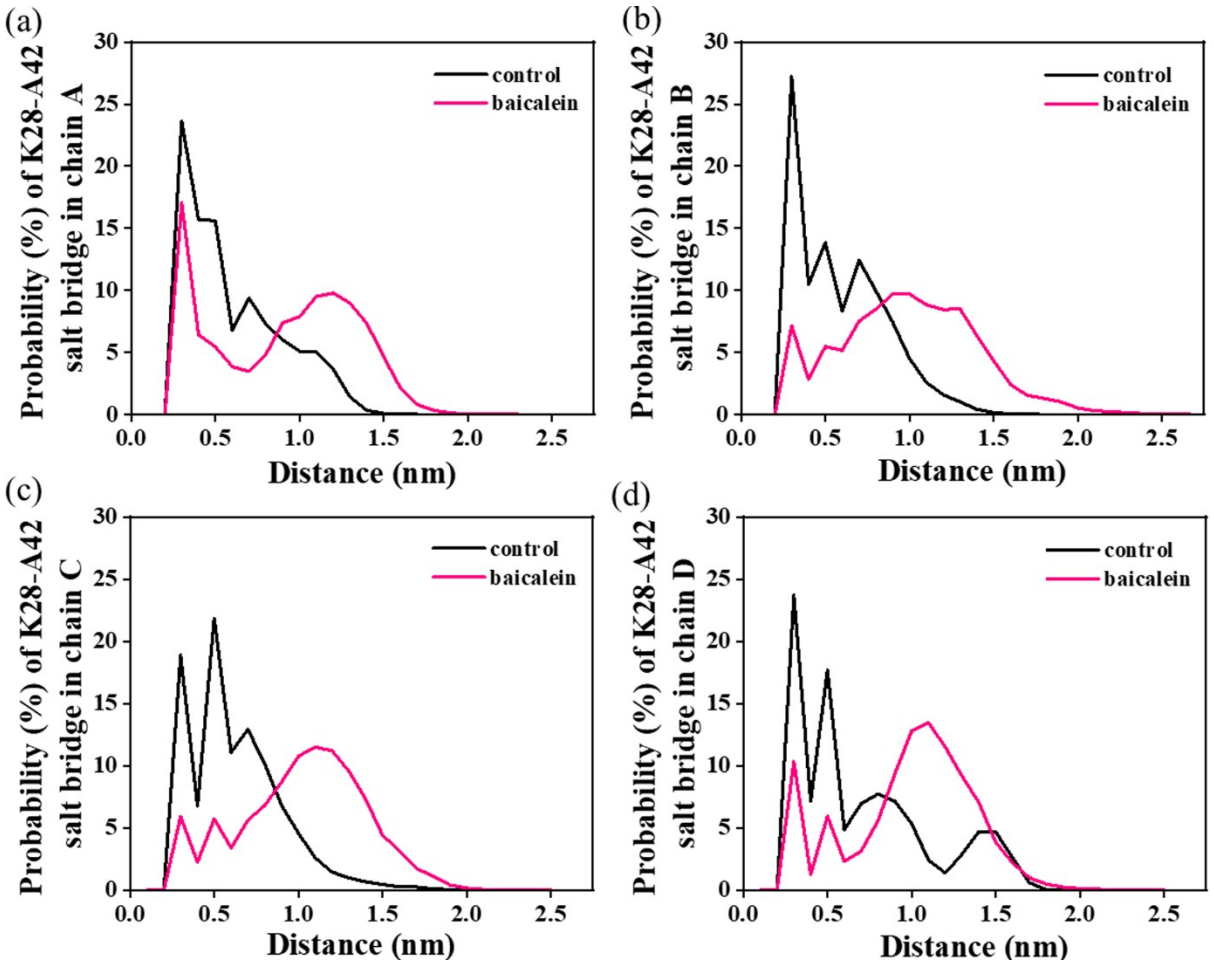

Figure S10: Distance distributions between K28 and A42 residues for salt bridge formation in control and baicalein systems.

Table S1: Molecular docking analysis of $A\beta_{42}$ protofibril-baicalein.

Compound	Protein[a]	AutoDock binding energy (kcal/mol)	$A\beta_{42}$ residues involved in intermolecular hydrogen bonds with baicalein			$A\beta_{42}$ residues involved in intermolecular hydrophobic contacts
			Residue	Atom[b]	Distance (nm)	
Baicalein	$A\beta_{42}$ protofibril	–6.9	Glu22(A) Glu22(A)	(4)O:NH (5)OH:O	0.29 0.29	Phe19(A), Phe20(A), Asp23(A), Val24(A), Asn27(A), Gly29(A)

[a]$A\beta_{42}$ protofibril (PDB ID: 5OQV); [b]Atoms on the left represent baicalein, and on the right represent $A\beta_{42}$ residue atoms.

Table S2: The $A\beta_{42}$ protofibril residues involved in intermolecular hydrophobic contacts with baicalein in the top nine docked poses.

Docked pose	AutoDock binding energy (kcal/mol)	$A\beta_{42}$ residues involved in intermolecular hydrophobic contacts with baicalein
1	–6.9	Phe19(A), Phe20(A), Asp23(A), Val24(A), Asn27(A), Gly29(A)
2	–6.2	Phe19(A), Ala21(A), Asn27(A), Gly29(A), Ala30(A), Ile31(A)
3	–6.0	Leu17(A), Phe19(A), Gly29(A), Ala30(A), Ile31(A)
4	–5.9	Phe19(A), Phe20(A), Glu22(A)
5	–5.8	Leu17(A), Val18(A), Phe19(A), Asn27(A), Gly29(A), Ala30(A), Ile31(A)
6	–5.8	Phe19(A), Phe20(A), Asn27(A), Gly29(A)
7	–5.6	Phe19(A), Phe20(A), Ala21(A), Val24(A), Asn27(A)
8	–5.5	Phe19(A), Ala21(A), Val24(A), Asn27(A), Gly29(A), Ile31(A)
9	–5.4	Phe19(A), Phe20(A), Glu22(A)

Table S3: Average number of hydrogen bonds during simulation between H6-E11 and E11-H13 of $A\beta_{42}$ protofibril in the two systems.

System	H6-E11	E11-H13
control	0.31 ± 0.10	0.25 ± 0.10
baicalein	0.02 ± 0.01	0.33 ± 0.12

Table S4: Secondary structure compositions of control and baicalein systems for repeat simulations.

Secondary structure component	control		baicalein	
	Simulation 1	Simulation 2	Simulation 1	Simulation 2
β-sheet[a]	60.7 ± 0.6	59.8 ± 0.7	56.7 ± 0.9	56.3 ± 0.5
Coil	25.7 ± 0.4	26.0 ± 0.3	29.9 ± 0.7	30.0 ± 0.6
Bend	12.0 ± 0.0	11.8 ± 0.4	11.2 ± 0.7	12.0 ± 0.4
Turn	0.3 ± 0.2	0.5 ± 0.2	0.0 ± 0.0	0.0 ± 0.0
Chain separator	2.0 ± 0.0	2.0 ± 0.0	2.0 ± 0.0	2.0 ± 0.0

[a]β-sheet= β-stand + β-bridge